


Article

The Influence of Nonthermal Plasma Technology on Oxidation Characteristics of Soot Operated on Direct Injection Internal Combustion Engines

Pichitpon Neamyu^{1,2}, Kampanart Theinnoi^{1,2,*} , Boonlue Sawatmongkhon^{1,2}, Thawatchai Wongchang^{2,3}, Chonlakarn Wongkhorsub^{1,2}, Sak Sittichompoo^{1,2} and Sathaporn Chuepeng⁴

¹ College of Industrial Technology, King Mongkut's University of Technology North Bangkok, 1518 Pracharat 1 Road, Wong Sawang, Bang Sue, Bangkok 10800, Thailand

² Research Centre for Combustion Technology and Alternative Energy (CTAE), Science and Technology Research Institute, King Mongkut's University of Technology North Bangkok, 1518 Pracharat 1 Road, Wong Sawang, Bang Sue, Bangkok 10800, Thailand

³ Department of Mechanical and Automotive Engineering Technology, Faculty of Engineering and Technology, King Mongkut's University of Technology North Bangkok (Rayong Campus), 19 Moo 11 Nong Lalok, Ban Khai, Rayong 21120, Thailand

⁴ ATAE Research Unit, Department of Mechanical Engineering, Faculty of Engineering at Sriracha, Kasetsart University, 199 Sukhumvit Road, Chonburi 20230, Thailand

* Correspondence: kampanart.t@cit.kmutnb.ac.th



Citation: Neamyu, P.; Theinnoi, K.; Sawatmongkhon, B.; Wongchang, T.; Wongkhorsub, C.; Sittichompoo, S.; Chuepeng, S. The Influence of Nonthermal Plasma Technology on Oxidation Characteristics of Soot Operated on Direct Injection Internal Combustion Engines. *Energies* **2022**, *15*, 9009. <https://doi.org/10.3390/en15239009>

Academic Editor: Andrzej Teodorczyk

Received: 31 October 2022

Accepted: 25 November 2022

Published: 28 November 2022

Publisher's Note: MDPI stays neutral with regard to jurisdictional claims in published maps and institutional affiliations.



Copyright: © 2022 by the authors. Licensee MDPI, Basel, Switzerland. This article is an open access article distributed under the terms and conditions of the Creative Commons Attribution (CC BY) license (<https://creativecommons.org/licenses/by/4.0/>).

Abstract: The combination of porous material with nonthermal plasma (NTP) technology to reduce the amount of particulate matter emitted from a direct-injection compression-ignition engine was investigated in this study. The investigation aimed at regulating particulate matter under long-term operation. A porous materials filter thickness of 4 mm was installed in the NTP reactor. The common rail diesel engine was fueled with 7%-vol biodiesel fuel (B7), and the experiment was carried out at steady-state conditions at 2000 rpm and indicated mean effective pressure (IMEP) of 6 bar. The effects of NTP high-voltage discharge (e.g., 2, 4, 5, 6, 8, and 10 kV) and the porous filter thickness (e.g., 0, 2, 4, and 6 mm) on particle number size distributions were examined. The prototype of combine porous filter and NTP illustrated good particulate removal (>70%) operated with a thickness of 4 mm of porous materials filter and a high voltage of 6 kV under the same power rating.

Keywords: soot; particulate matter; diesel particulate filter; non-thermal plasma; porous material; particle number size distributions; diesel engine emission

1. Introduction

Diesel engines have high emissions of particulate matter emissions (PM). PM in the exhaust gas results from the combustion process. It originates from the accumulation of very small particles of partly burned fuel, partly burned lube oil, ash content of fuel oil, and cylinder lube oil or sulfates and water, posing a significant threat to environmental protection and human health [1–3]. Therefore, the catalytic diesel particulate filter (CDPF) has been acclaimed as a potential technique for reducing soot emissions since the presence of catalysts may effectively reduce the ignition temperature of soot and prolong the CDPF's low back pressure [4–6]. Creating very effective catalysts for soot oxidation was crucial for CDPF technology. Noble metals, transition metal oxides, perovskite catalysts, and spinel catalysts are the principal subjects of current research on soot oxidation catalysts [5,7]. According to Stpie et al., Ce addition could both lower PM emissions and enhance the regeneration of the DPF by catalytic PM burning [8]. After numerous DPF regeneration cycles, Pérez et al. [9] evaluated the actions of the Ce-based and Pt active phases and discovered that, under most circumstances, they were regenerated at the same temperature. In order to accelerate soot oxidation, Murota et al. [10] demonstrated that when the temperature

hits 400 °C, the gaseous oxygen may exchange oxygen with the CeO₂ lattice oxygen and generate 77 active oxygen species in the process. Researchers found that the inclusion of heterogeneous catalysts might lower the ignition temperature of soot to 400–450 °C, which is still much greater than the temperature of diesel engine exhaust, particularly during the start-up phase and the regular operation of diesel engines (below 200–300 °C) [11,12]. Therefore, it is vitally necessary to find a solution that allows soot to oxidize at a relatively low temperature.

Nonthermal plasma (NTP) technology has been identified as one of the most promising contemporary approaches to the problem of diesel exhaust pollution. Plasma comprises various electrons, ions, and neutral particles, considered the fourth state of matter [13]. The non-thermal plasma (NTP) was used for after-treatment in the exhaust gas in the diesel engine because the formation of electron property promotes the decomposition of exhaust gases [13,14]. During NTP reactions, the amount of PM significantly decreased, and the surface's stacking structure shifted from a convex blocky or spherical structure to a relatively smooth surface [15]. Babaie et al. [16] used diluted diesel exhaust to a dielectric barrier discharge reactor and generated plasma using a high-voltage discharge to study the decomposition of PM. PM had the highest mass removal effectiveness at 43.9%. Several research teams have investigated the use of nonthermal plasma (DBD) to reduce particulate matter PM and NO_x emissions from diesel exhaust [17–19]. The results showed that 90% of PM was removed by non-thermal plasma (NTP) [20]. Fushimi et al. [18], in experiments on several NTP reactor designs to remove PM, found that the primary products of PM oxidation and breakdown were CO and CO₂. At the same time, active chemicals that played significant roles were O₃ and NO₂. Wang et al. [21,22] researched how a dielectric barrier discharge NTP generator affected PM's physical and chemical properties in a diesel engine exhaust. The degree of aggregation and the mean spherule diameters of PM was significantly decreased, according to the results. In addition, after NTP treatment, the number of carbon atoms in PM was significantly decreased while the amount of other metal components was almost unchanged. Gao et al. [23] conducted an analysis of the nanostructures of PM released from a diesel engine fitted with an NTP after-treatment system. Regardless of engine loads, partial oxidation decreased the primary diameter of PM and the empty cores. Core-shell-like structures broke down into tightly packed fringe bands towards the conclusion of PM oxidation.

The research aimed to study the combined effect between porous material and NTP technology impact on the particulate mass and particulate number from the internal combustion engine using biodiesel fuel as a main fuel.

2. Materials and Methods

2.1. Exhaust Particle Size

Figure 1 shows the schematic diagram of the experimental setup in this paper. It consists of a diesel engine model ISUZU 4JK-1TC (standard commercial EURO 4), exhaust pipes, DPF, a non-thermal plasma reactor, and an EEPS-3090 (Engine Exhaust Particle Sizer Spectrometer 3090, TSI Inc., Shoreview, MN, USA). The ISUZU 4JK-1TC engine is popular in Thailand and is a high-PM-emission engine. The main engine specifications are shown in Table 1. In the test first step, the diesel engine was warmed up with exhaust vented through valve 1 because internal combustion engines operate most efficiently at relatively high temperatures, typically above 80–90 °C. Then, the DPF was tested at a speed of 2000 r/min and indicated mean effective pressure (IMEP) 6 bar Through valve 2. Then, the DPF with non-thermal plasma (NTP) through valve 3. The EEPS measured the exhaust particle size distribution and number concentration before and after DPF.

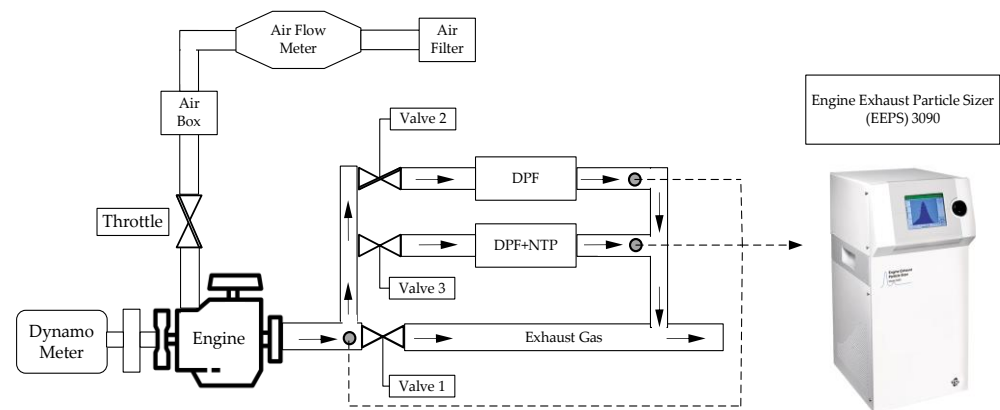


Figure 1. Schematic diagram of the experimental setup.

Table 1. Engine specification of the 4JK-1TC model.

Engine Parameter	Specifications
No of cylinder	4
Fuel injection	Common-rail DI
Displacement volume (cm ³)	2499
Bore × Stroke (mm)	95.4 × 87.4
Compression ratio	18.1
Maximum power (kW)	87@1800–2200 rpm
Maximum torque (Nm)	280@1800–2200 rpm
Fuel	Biodiesel

2.2. Nonthermal Plasma Reactor

Figure 2 shows a diagram of non-thermal plasma (NTP) with DPF system. It is a DBD-type NTP reactor consisting of a barrier of internal and external electrodes. Internal was composed of the DPF. First, the DPF layer was changed from 2, 4, and 6 mm using a nickel foam material shown in Figure 3. Next, with a copper cylinder structure diameter of 19 mm. The barrier was a quartz tube with an inner diameter of 20 mm and a wall thickness of 1.5 mm. The external electrode was a stainless cylinder with an inner diameter of 26 mm. The thickness of the discharge gap between the quartz tube and the internal electrode was 1.5 mm. with an outer diameter of 63.5 mm. with a plasma discharge zone length of 70 mm. The electric parameter measurement system was composed of a high-voltage amplifier (Trek 10/10B-HS, Advanced Energy Industries, Inc. Output Voltage 0 to ±10 kV DC or Peak AC adjustable) and a digital oscilloscope (DSOX1204G, Keysight Technologies, Santa Rosa, CA, USA). The high-voltage amplifier was used to supply power for the NTP system, and the oscilloscope was used to monitor the discharge conditions. Non-thermal plasma (NTP) was examined at applied voltages of 0, 2, 4, 5, 6, 8, and 10 kV at 500 Hz.

Space velocity (SV) was the ratio between the gas flow rate through the DPF standard commercial and the plasma reactor effective volume of the reactor, as shown in Equation (1):

$$SV = \frac{Q_{gas}}{V_{eff}} (h^{-1}), \quad (1)$$

where space velocity (SV) was composed, Q_{gas} is the exhaust gas flow rate in the plasma reactor (m³/h) and V_{eff} is volume of the plasma reactor effective length (m³).

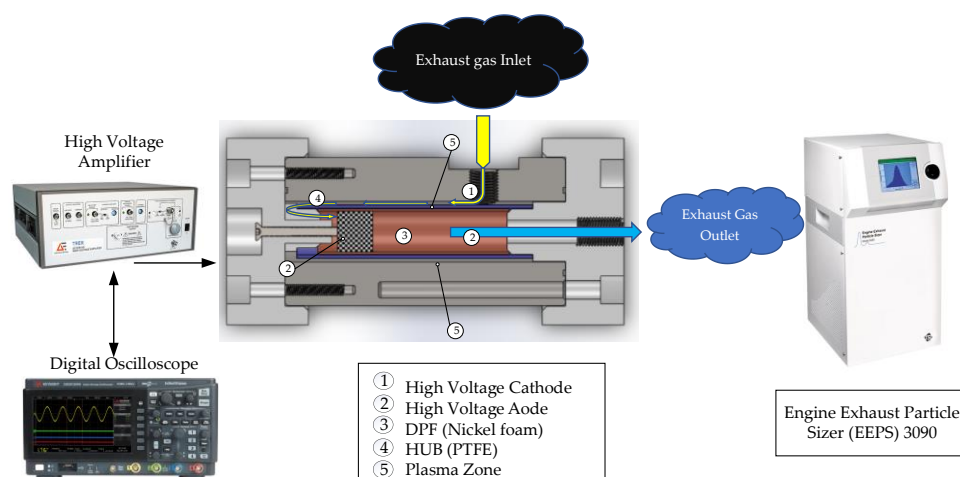


Figure 2. Diagram of Non-thermal plasma (NTP) with Porous Material.



Figure 3. The Porous Material.

The porous material properties are shown in Table 2. The experimental material used the commercial nickel foam that had the properties as the following number of holes (13–120 ($\pm 5 \times 10$) ppi), area density (280 g/m²), thickness (2, 4, 6 mm) and diameter (18 mm).

Table 2. Specification of Porous material.

Engine Parameter	Specifications
Material	Nickel foam
Number of holes (PPI)	13–120 ($\pm 5 \times 10$)
Area density (g/m ²)	280
Thickness (mm)	2, 4, 6
Diameter (mm)	18

2.3. Mechanism of NTP Technology on Particulate Matter (PM)

When high voltage was applied to the reactor, large amounts of electrons were in the plasma zone. As a result, O₂ and H₂O in the exhaust were converted to OH and O radicals by colliding with the electrons (Equations (2) and (3)). O combined with O₂ converted to ozone O₃ (Equation (4)). Soot in the exhaust was oxidation to CO and CO₂ from the reaction of ozone, OH, and O (Equations (5)–(10)), which could be PM oxidation in the NTP discharge. The oxidation of CO by OH radicals was represented by Equation (11). As the main components of SOF in the PM, HC combined with O and O₃ to form CO₂ (Equations

(12) and (13)) as shown in Figure 4. Therefore, PM could be efficiency decreased under the NTP treatment due to a reaction with the high oxidative [24,25].

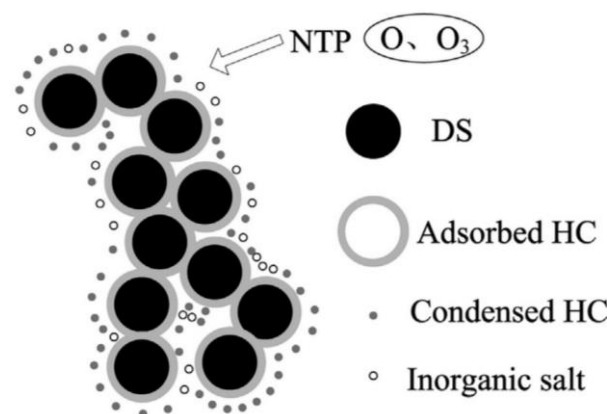
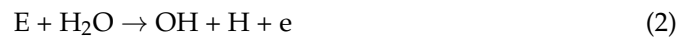


Figure 4. Decomposition of the PM in the NTP reaction model [15].

3. Result and Discussion

3.1. Effect of Non-Thermal Plasma (NTP) without Porous Material (0 mm)

Figure 5a showed the particle number size distributions of diesel exhaust measured using an engine exhaust particle sizer spectrometer (EEPS) without the non-thermal plasma (NTP) and porous material under 6 IMEP engine load with a dilution ratio of 8. In Figure 5, the black line datasets show the particle sizer of the exhaust engine out and the dash line data set shows data by applying a high voltage of 2, 4, 5, 6, 8, and 10 kV as a cases study of the effect of NTP on particle number size distributions. The pulse frequency is 500 Hz. The results show that the high voltage of non-thermal plasma (NTP) can significantly reduce PM because the electrons in the plasma state were used for the reaction with emissions in the exhaust gas which promote the reduction of PM [26]. The mechanism of NTP technology on particulate matter (PM) is shown in Equations (2)–(13) [27–29]. However, the plasma had fewer effects on particle size distribution (PM) compared with the engine out in the range of 25–130 nm. In other words, the comparison of all high voltage shows the deceased of the particle mass concentrations when increasing the high voltage, as shown in Figure 5b.

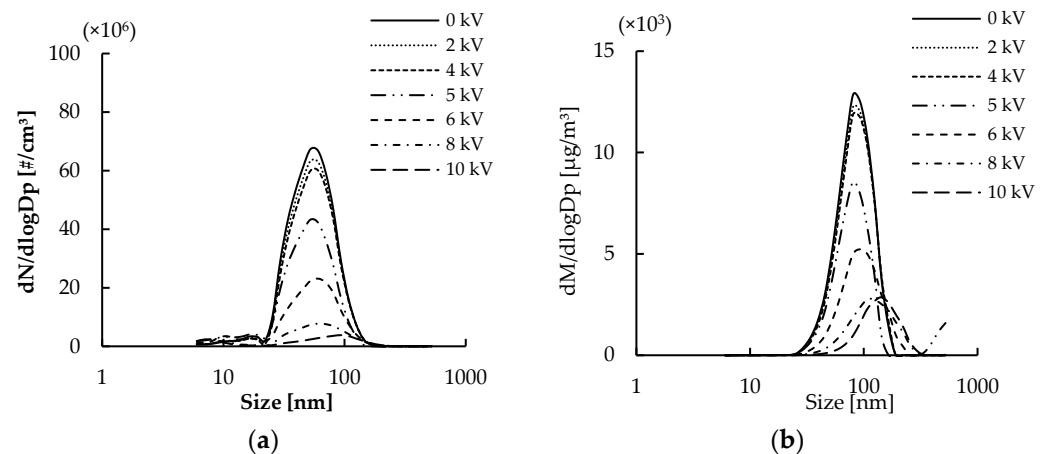


Figure 5. Average number-mass size distributions of PM without Porous Material and NTP when (a) Particle number size distributions; (b) Particle Mass size distributions.

Figure 6 shows the PM emissions using in units of percentage. The particulate matter (PM) of the engine out of values is 67.32 million ($dN/dlogDp$ [$\#/cm^3$]), equivalent to 100%. The comparison applied voltages of 0, 2, 4, 6, 8, and 10 kV at 500 Hz. This experimental results in particle number reduction values of 6%, 10%, 35%, 65%, 88% and 94% respectively. It was not that the results obtained from the experiments at HV plasma 5 and 6 kV were able to significantly reduce small blast dust of 25% and 30% when considering differences from HV 2, 4, 5, 8, and 10 kV. Because larger particles are more easily charged and removed via electrostatic precipitation, the device is probably more effective for larger particles, which are the noticeable shifts in particle size distribution to smaller diameters [30]. Plasma affects the particulate removal in terms of input of the ionization energy into the exhaust gas which results in the reduction of particulate because the electron promotes hydroxide radicals (OH^*), oxygen radicals (O^*), and ozone (O_3) following Equations (2)–(4). The removal of particulate because of the reaction of particulate (Carbon) with O^* , O_3 , and OH^* results in CO, CO_2 , and H^* following Equations (5)–(11). The change of C to CO and CO_2 caused the decrease in particulate. The ionization energy was increased when rising the HV was 2 to 10 kV.

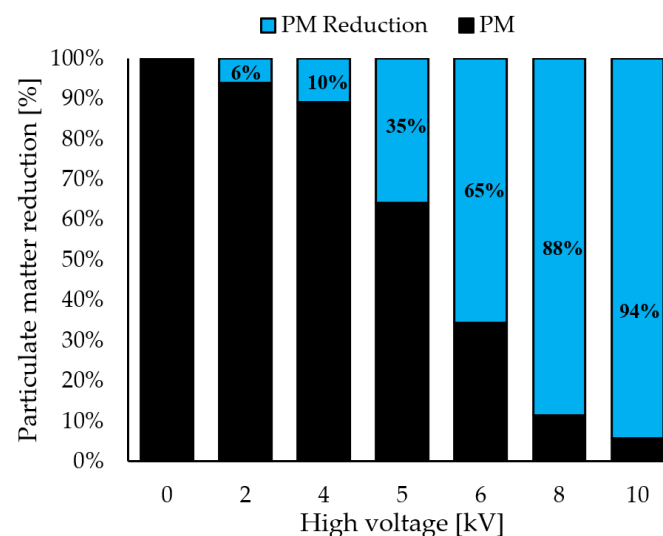


Figure 6. The reduction of Particle number without Porous Material and NTP.

3.2. Effect of Porous Material without Non-Thermal Plasma (NTP)

Figure 7a shows the Particle number size distributions of diesel exhaust measured using an engine exhaust particle sizer spectrometer (EEPS) with porous material and

without the non-thermal plasma (NTP) under 6 IMEP engine load with a dilution ratio of 8. In this Figure, the black line dataset shows the pure engine exhaust particle sizer. The dotted line dataset shows data using porous material thicknesses of 2, 4, and 6 mm. It was found that porous materials of all thicknesses could reduce the amount of PM with a number in the 22–150 nm range in all conditions. However, at 2 mm porous material has effect on the PM trapping slightly decrease around 4%, but with an increase in porous material thicknesses of 4 and 6 mm, PM trapping was significantly effective. which could be reduced by 24 and 26% respectively. Considering the cost-effectiveness of the application, 4 mm is an attractive option as 6 mm. can reduce PM no different from 4 mm, including Mass concentration distributions shown in Figure 7b.

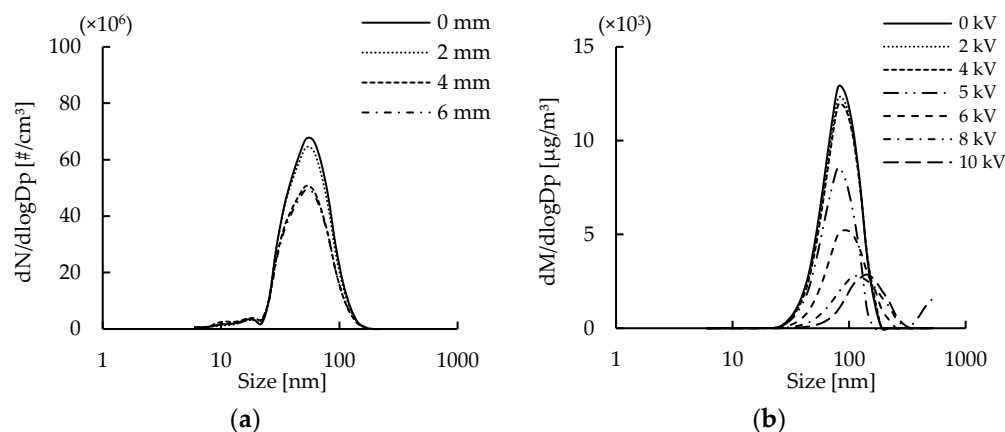


Figure 7. Average number-mass size distributions of PM with Porous Material and without NTP when (a) Particle number size distributions; (b) Particle Mass size distributions.

Figure 7a shows the particle number size distributions of diesel exhaust measured using an engine exhaust particle sizer spectrometer (EEPS) with porous material and without the non-thermal plasma (NTP) under 6 IMEP engine load with a dilution ratio of 8. In this as Figure 7, the black line dataset shows the pure engine exhaust particle sizer. The dotted line dataset shows data using porous material thicknesses of 2, 4, and 6 mm. It was found that porous materials of all thicknesses could reduce the amount of PM with a number in the 22–150 nm range in all conditions. However, at 2 mm porous material has effect on the PM trapping slightly decrease around 4%, but with an increase in porous material thicknesses of 4 and 6 mm, PM trapping was significantly effective. which could be reduced by 24 and 26% respectively. Considering the cost-effectiveness of the application, 4 mm is an attractive option as 6 mm. can reduce PM no different from 4 mm, including Mass concentration distributions shown in Figure 7b.

Figure 8 shows the PM emissions using in units of percentage. Here, the particulate matter (PM) of the engine out of values is 67.32 million ($dN/d\log D_p$ [$\#/\text{cm}^3$]), equivalent to 100%. Compare applying a porous material thickness of 2, 4, and 6 mm. This experimental results in particle reductions of 4%, 24%, and 26% respectively. In addition, soot deposition is also influenced by filter geometry, including filter volume, cell density, and wall thickness, as well as pore microstructure, including porosity, pore size/size distribution, and pore connectivity [31].

3.3. Effect of Porous Material with Non-Thermal Plasma (NTP)

The results of previous experiments used these data to select a porous material thickness of 4 mm. In testing with NTP at high voltages of 2, 4, 6, 5, 6, 8, and 10 kV, NTP was able to reduce the number of PMs by 3%, 11%, 24%, 72%, 90%, and 94%, respectively. However, the interesting point is that high voltage at 6 kV can significantly reduce PM due to the reduced number of PM. That is 72% compared to other high voltage. The influencers of PM reduction were the energy of NTP and porous material which encourage better cooperation to promote the reduction of PM shown in Figure 9.

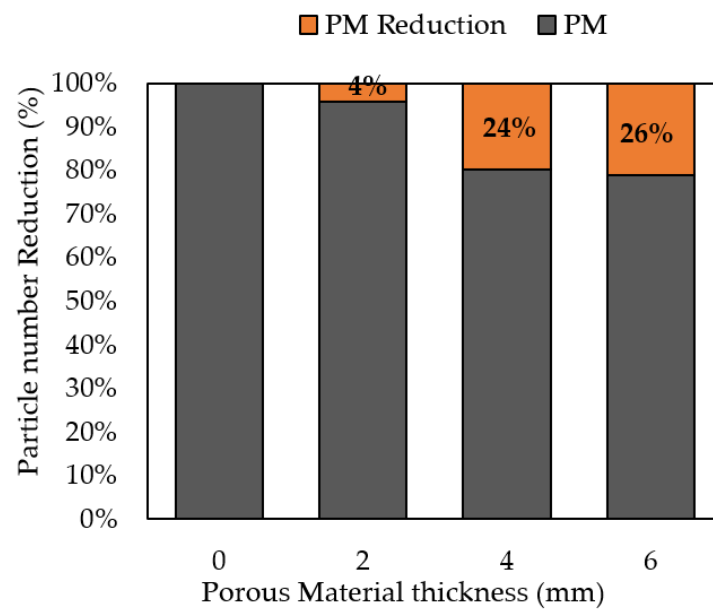


Figure 8. The reduction of Particle number with Porous Material and without NTP.

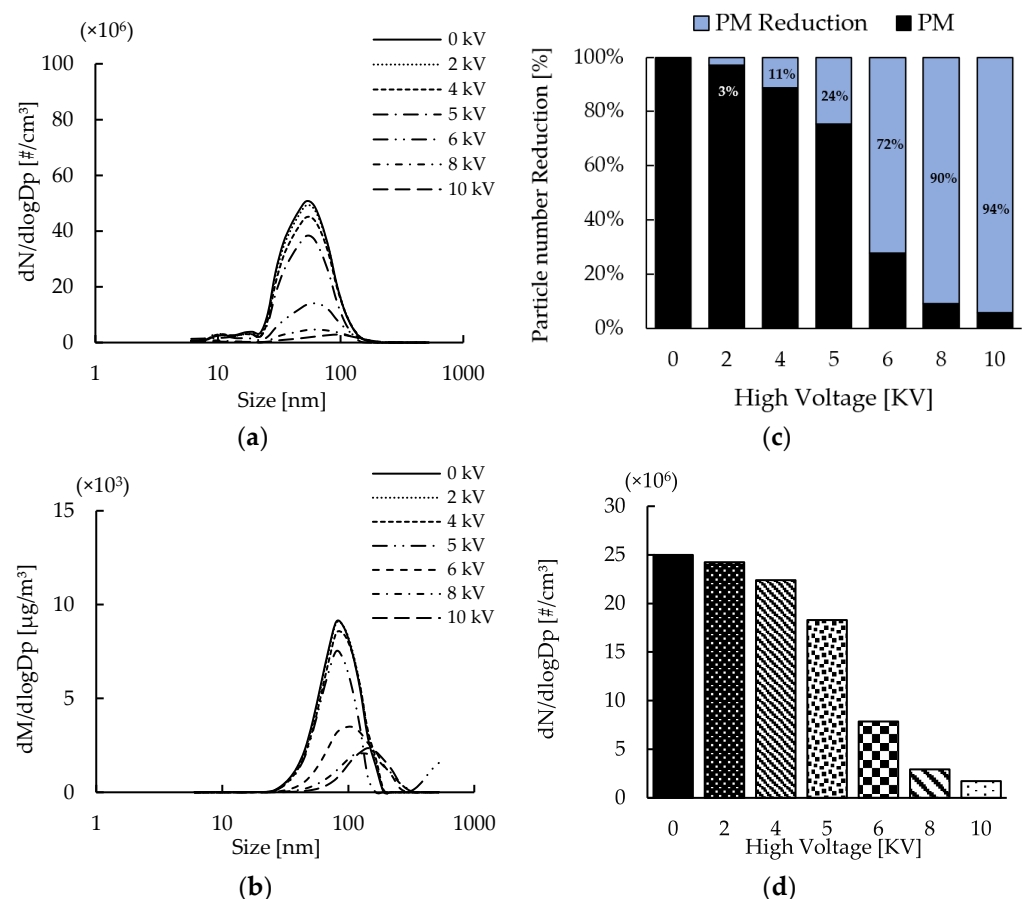


Figure 9. Average number-mass size distributions of PM using the combination of porous material 4 mm and NTP (a) Particle number size distributions; (b) Particle Mass size distributions. The reduction of PM with the combination of porous material 4 mm and NTP when (c) percentage and (d) Particle Number.

The energy of PM reduction was shown in Figure 10. This figure present to explains the energy of plasma to use reduce the particle mass of PM. It showed the reduction in the

particle mass of PM when increases the input energy. The case of high voltage at 0–4 kV showed less of decreasing in particle mass of PM. The high voltage at 6–10 kV shows a high reduction of particle mass of PM. Moreover, the energy (J) for promote the electron of plasma in case of 6 kV shows the significant reducing of particle mass of PM that showed in Figure 10. Therefore, it can be available the energy to promote the PM reduction for a porous material thickness of 4 mm because the injection of ions at a direct current below the corona discharge/ionization threshold causes the remediation to increase between 0 and 5 kV pulse voltage which is lower than a pulse voltage cutoff of Ion density is not high enough at 5 kV to cause electrostatic precipitation. Similarly, there is inadequate power available below a DC voltage of 2 kV to remove the charged nanoparticles using electrostatic force-restricted time spent within the coaxial reactor.

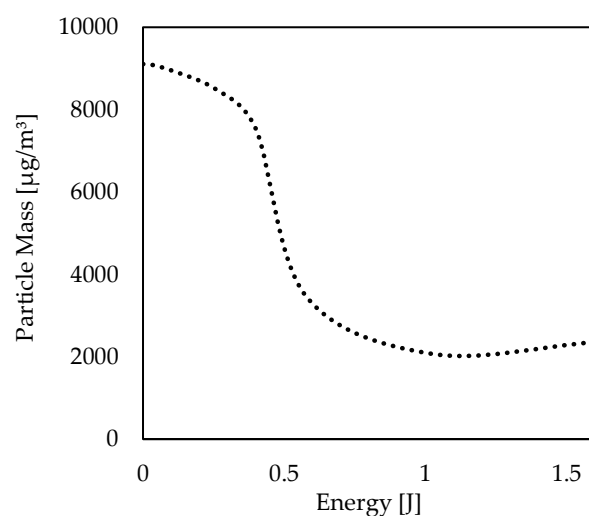


Figure 10. The conversion of Energy to effect PM reduction.

4. Conclusions

This research shows the efficiency to reduce the amount of PM from internal combustion engines. The NTP treatment system combined with the porous materials result in the 6 kV input for high voltage with 4 mm thickness porous material show the best particulate removal efficiency (up to 72%) compared with high-voltage input (8 and 10 kV) under the same power rating. The main influence on remove of particulate size seems to be influenced not only by the NTP, but also by the porous material. However, the optimized operating system to assist NTP and porous filter activities to understand this effect are required for better particulate matter activity.

Author Contributions: Conceptualization, B.S.; Methodology, T.W.; Formal analysis, C.W.; Investigation, P.N.; Resources, S.C.; Writing—original draft, P.N.; Writing—review & editing, K.T. and S.S.; Supervision, K.T. and C.W. All authors have read and agreed to the published version of the manuscript.

Funding: This research was funded by the College of Industrial Technology, King Mongkut's University of Technology North Bangkok (grant No. Res-CIT0287/2022).

Conflicts of Interest: The authors declare no conflict of interest.

References

1. Prasad, R.; Singh, S.V. A review on catalytic oxidation of soot emitted from diesel fuelled engines. *J. Environ. Chem. Eng.* **2020**, *8*, 103945. [[CrossRef](#)]
2. Feng, X.; Ge, Y.; Ma, C.; Tan, J.; Yu, L.; Li, J.; Wang, X. Experimental study on the nitrogen dioxide and particulate matter emissions from diesel engine retrofitted with particulate oxidation catalyst. *Sci. Total Environ.* **2014**, *472*, 56–62. [[CrossRef](#)] [[PubMed](#)]
3. Reşitoğlu, İ.A.; Altinişik, K.; Keskin, A. The pollutant emissions from diesel-engine vehicles and exhaust aftertreatment systems. *Clean Technol. Environ. Policy* **2015**, *17*, 15–27. [[CrossRef](#)]

4. Ou, J.; Meng, Z.; Hu, Y.; Du, Y. Experimental investigation on the variation characteristics of soot layer thickness and pressure drop during DPF/CDPF active regeneration. *Chem. Eng. Sci.* **2021**, *241*, 116682. [\[CrossRef\]](#)
5. Mishra, A.; Prasad, R. Preparation and application of perovskite catalysts for diesel soot emissions control: An overview. *Catal. Rev. Sci. Eng.* **2014**, *56*, 57–81. [\[CrossRef\]](#)
6. Zhu, X.; Wu, H.; Luo, J.; Liu, J.; Yan, J.; Zhou, Z.; Yang, Z.; Jiang, Y.; Chen, G.; Yang, G. Soot Oxidation in a Plasma-Catalytic Reactor: A Case Study of Zeolite-Supported Vanadium Catalysts. *Catalysts* **2022**, *12*, 677. [\[CrossRef\]](#)
7. Dhal, G.C.; Mohan, D.; Prasad, R. Preparation and application of effective different catalysts for simultaneous control of diesel soot and NOx emissions: An overview. *Catal. Sci. Technol.* **2017**, *7*, 1803–1825. [\[CrossRef\]](#)
8. Stępień, Z.; Ziemiański, L.; Żak, G.; Wojtasik, M.; Jęczmionek, Ł.; Burnus, Z. The evaluation of fuel borne catalyst (FBC's) for DPF regeneration. *Fuel* **2015**, *161*, 278–286. [\[CrossRef\]](#)
9. Pérez, V.R.; Bueno-López, A. Catalytic regeneration of Diesel Particulate Filters: Comparison of Pt and CePr active phases. *Chem. Eng. J.* **2015**, *279*, 79–85. [\[CrossRef\]](#)
10. Murota, T.; Hasegawa, T.; Aozasa, S.; Matsui, H.; Motoyama, M. Production method of cerium oxide with high storage capacity of oxygen and its mechanism. *J. Alloys Compd.* **1993**, *193*, 298–299. [\[CrossRef\]](#)
11. Mori, K.; Miyauchi, Y.; Kuwahara, Y.; Yamashita, H. Shape effect of MnOx-decorated CeO₂ Catalyst in the Diesel Soot Oxidation. *Bull. Chem. Soc. Jpn.* **2017**, *90*, 556–564. [\[CrossRef\]](#)
12. Liu, J.; Yang, J.; Sun, P.; Ji, Q.; Meng, J.; Wang, P. Experimental investigation of in-cylinder soot distribution and exhaust particle oxidation characteristics of a diesel engine with nano-CeO₂ catalytic fuel. *Energy* **2018**, *161*, 17–27. [\[CrossRef\]](#)
13. Gomez, E.; Rani, D.A.; Cheeseman, C.; Deegan, D.; Wise, M.; Boccaccini, A. Thermal plasma technology for the treatment of wastes: A critical review. *J. Hazard. Mater.* **2009**, *161*, 614–626. [\[CrossRef\]](#)
14. Song, C.-L.; Bin, F.; Tao, Z.-M.; Li, F.-C.; Huang, Q.-F. Simultaneous removals of NOx, HC and PM from diesel exhaust emissions by dielectric barrier discharges. *J. Hazard. Mater.* **2009**, *166*, 523–530. [\[CrossRef\]](#)
15. Shi, Y.; Cai, Y.; Li, X.; Ji, L.; Chen, Y.; Wang, W. Evolution of diesel particulate physicochemical properties using nonthermal plasma. *Fuel* **2019**, *253*, 1292–1299. [\[CrossRef\]](#)
16. Babaie, M.; Kishi, T.; Arai, M.; Zama, Y.; Furuhashi, T.; Ristovski, Z.; Rahimzadeh, H.; Brown, R.J. Influence of non-thermal plasma after-treatment technology on diesel engine particulate matter composition and NOx concentration. *Int. J. Environ. Sci. Technol.* **2015**, *13*, 221–230. [\[CrossRef\]](#)
17. Fushimi, C.; Madokoro, K.; Yao, S.; Fujioka, Y.; Yamada, K. Influence of polarity and rise time of pulse voltage waveforms on diesel particulate matter removal using an uneven dielectric barrier discharge reactor. *Plasma Chem. Plasma Process.* **2008**, *28*, 511–522. [\[CrossRef\]](#)
18. Vinh, T.Q.; Watanabe, S.; Furuhashi, T.; Arai, M. Effects of particulate matter on NOx removal in dielectric barrier discharges. *J. Energy Inst.* **2012**, *85*, 163–169. [\[CrossRef\]](#)
19. Kuwahara, T.; Yoshida, K.; Kuroki, T.; Hanamoto, K.; Sato, K.; Okubo, M. Pilot-Scale Combined Reduction of Accumulated Particulate Matter and NOx Using Nonthermal Plasma for Marine Diesel Engine. *IEEE Trans. Ind. Appl.* **2019**, *56*, 1804–1814. [\[CrossRef\]](#)
20. Yao, S.; Kodama, S.; Yamamoto, S.; Fushimi, C.; Madokoro, K.; Mine, C.; Fujioka, Y. Characterization of an uneven DBD reactor for diesel PM removal. *Asia-Pac. J. Chem. Eng.* **2009**, *5*, 701–707. [\[CrossRef\]](#)
21. Wang, P.; Gu, W.; Lei, L.; Cai, Y.; Li, Z. Micro-structural and components evolution mechanism of particulate matter from diesel engines with non-thermal plasma technology. *Appl. Therm. Eng.* **2015**, *91*, 1–10. [\[CrossRef\]](#)
22. Wang, P.; Cai, Y.X.; Zhang, L.; Tolsdorf, C. Physical and chemical characteristics of particulate matter from biodiesel exhaust emission using non-thermal plasma technology. *Energy Fuels* **2010**, *24*, 3195–3198. [\[CrossRef\]](#)
23. Gao, J.; Ma, C.; Xing, S.; Sun, L.; Huang, L. Nanostructure analysis of particulate matter emitted from a diesel engine equipped with a NTP reactor. *Fuel* **2017**, *192*, 35–44. [\[CrossRef\]](#)
24. Matti Maricq, M. Chemical characterization of particulate emissions from diesel engines: A review. *J. Aerosol Sci.* **2007**, *38*, 1079–1118. [\[CrossRef\]](#)
25. Zhu, K.; Cai, Y.; Shi, Y.; Lu, Y.; Zhou, Y.; He, Y. The effect of nonthermal plasma on the oxidation and removal of particulate matter under different diesel engine loads. *Plasma Process. Polym.* **2021**, *19*, 2100104. [\[CrossRef\]](#)
26. Vandenbroucke, A.M.; Morent, R.; de Geyter, N.; Leys, C. Non-thermal plasmas for non-catalytic and catalytic VOC abatement. *J. Hazard. Mater.* **2011**, *195*, 30–54. [\[CrossRef\]](#) [\[PubMed\]](#)
27. Zheng, Q.; Zhao, Z.; Zuo, J.; Yang, J.; Wang, H.; Yu, S.; Yi, D. A comparative study: Early results and complications of percutaneous and surgical closure of ventricular septal defect. *Cardiology* **2009**, *114*, 238–243. [\[CrossRef\]](#) [\[PubMed\]](#)
28. Magne, L.; Pasquiers, S. LIF spectroscopy applied to the study of non-thermal plasmas for atmospheric pollutant abatement. *Comptes Rendus Phys.* **2005**, *6*, 908–917. [\[CrossRef\]](#)
29. Takaki, K.; Hatanaka, Y.; Arima, K.; Mukaigawa, S.; Fujiwara, T. Influence of electrode configuration on ozone synthesis and microdischarge property in dielectric barrier discharge reactor. *Vacuum* **2008**, *83*, 128–132. [\[CrossRef\]](#)

-
30. Yang, S.; Aravind, I.; Zhang, B.; Weng, S.; Zhao, B.; Thomas, M.; Umstattd, R.; Singleton, D.; Sanders, J.; Cronin, S.B. Plasma-enhanced electrostatic precipitation of diesel exhaust using high voltage nanosecond pulse discharge. *J. Environ. Chem. Eng.* **2021**, *9*, 106565. [[CrossRef](#)]
 31. Choi, S.; Oh, K.-C.; Lee, C.-B. The effects of filter porosity and flow conditions on soot deposition/oxidation and pressure drop in particulate filters. *Energy* **2014**, *77*, 327–337. [[CrossRef](#)]